



CrossMark  
click for updates

Cite this: *RSC Adv.*, 2015, 5, 64220

# Rationalizing the role of the anion in CO<sub>2</sub> capture and conversion using imidazolium-based ionic liquid modified mesoporous silica†

A. S. Aquino,<sup>ab</sup> F. L. Bernard,<sup>ab</sup> J. V. Borges,<sup>b</sup> L. Mafrá,<sup>c</sup> F. Dalla Vecchia,<sup>b</sup> M. O. Vieira,<sup>ab</sup> R. Ligabue,<sup>ab</sup> M. Seferin,<sup>ab</sup> Vitaly V. Chaban,<sup>d</sup> E. J. Cabrita<sup>e</sup> and S. Einloft<sup>\*ab</sup>

Covalently supported ionic liquids in mesoporous materials were prepared by grafting 1-methyl-3-(3-trimethoxysilylpropyl)imidazolium chloride in MCM-41. Subsequently, the [Cl<sup>-</sup>] anion was changed to [BF<sub>4</sub><sup>-</sup>], [PF<sub>6</sub><sup>-</sup>] or [Tf<sub>2</sub>N<sup>-</sup>]. These materials that present an advantageous combination of the properties of mesoporous solid materials and ionic liquids were evaluated for CO<sub>2</sub> sorption as well as catalysts for CO<sub>2</sub> conversion into cyclic carbonate using propylene oxide. The material with the [Cl<sup>-</sup>] anion had the best performance for both CO<sub>2</sub> sorption and conversion. A CO<sub>2</sub> sorption of 11 w/w% on the adsorbent was achieved and the cycloaddition reaction exhibited a conversion of 67% with 82% selectivity with the catalyst remaining active after 5 cycles, proving that the same sorbent/catalyst setup can be used for both CO<sub>2</sub> capture and conversion. Based on the experimental data and electronic-structure numerical simulations, we have hypothesized two major reasons why chloride out performs other anions when adsorbed on MCM-41 unlike unsupported ionic liquids.

Received 25th April 2015

Accepted 21st July 2015

DOI: 10.1039/c5ra07561k

[www.rsc.org/advances](http://www.rsc.org/advances)

## Introduction

The mitigation scenario for CO<sub>2</sub> emissions is mainly based on the efficient energy use, the substitution of fossil fuels by renewable energy sources, as well as in the improvement/development of carbon capture and storage (CCS) technologies. The major drawbacks for carbon dioxide reinjection in geological sites are largely related to the involved energy penalty leading to high costs. A carbon capture and utilization (CCU) concept has recently emerged, where captured CO<sub>2</sub> is not considered as waste but rather a C1 building block for various chemicals,<sup>1</sup> thus demanding the development of new processes and materials that can perform both carbon capture and chemical conversion. Since organic carbonates can be used for

various purposes, such as polar aprotic solvents, intermediates in organic synthesis, monomers for polycarbonate synthesis, among others,<sup>2</sup> cyclic carbonates appeared as one of the important choices for CO<sub>2</sub> utilization from its cycloaddition to epoxides. The use of ionic liquids (ILs) as solvents in processes for CO<sub>2</sub> separation from flue gas is well described in the literature<sup>3-6</sup> as well as their use as catalysts for CO<sub>2</sub> conversion into cyclic carbonates.<sup>7-10</sup> The synergistic effects of ionic liquids as catalysts for CO<sub>2</sub> cycloaddition to epoxides has been recently reviewed<sup>11</sup> and Sun and Zhang has demonstrated the role of Cl<sup>-</sup> anion as a nucleophilic agent, by a density functional theory study, when ionic liquids are used as catalysts for this reaction.<sup>12</sup>

Nevertheless, there are still some technological challenges for the adoption of ILs in CCS and CCU technologies, specially related to the typical high viscosities presented by ILs. The integration of ionic liquids into solid matrices appears as a promising solution for this trouble, as heterogeneous systems are cheaper, more suitable for reactors design and separation steps. This alternative also retains the advantages of ILs, as green solvents due to the low vapor pressure, high chemical and thermal stability and recyclability.<sup>13</sup>

The solids commonly used in CO<sub>2</sub> capture are zeolites, activated carbon (ACs),<sup>14</sup> carbon molecular sieves (CMS),<sup>15</sup> metal-organic frameworks (MOFs),<sup>16</sup> mesoporous silicas, polymeric or inorganic membranes<sup>15</sup> and currently mixed matrix membranes with the incorporation of zeolites in polymeric membranes.<sup>17</sup>

<sup>a</sup>Programa de Pós-Graduação em Engenharia e Tecnologia de Materiais (PGETEMA) – Pontifícia Universidade Católica do Rio Grande do Sul (PUCRS), Porto Alegre, Brazil. E-mail: einloft@puers.br

<sup>b</sup>Faculdade de Química (FAQUI) – Pontifícia Universidade Católica do Rio Grande do Sul (PUCRS), Porto Alegre, Brazil

<sup>c</sup>Departamento de Química, Universidade de Aveiro, Campus de Santiago, CICECO, Aveiro, Portugal

<sup>d</sup>Instituto de Ciência e Tecnologia, Universidade Federal de São Paulo, 12231-280, São José dos Campos, SP, Brazil

<sup>e</sup>REQUIMTE, UCIBIO, Departamento de Química, Faculdade de Ciências e Tecnologia, 2829-516 Caparica, Portugal

† Electronic supplementary information (ESI) available: FTIR absorption bands of IL and supported IL, TGA thermogram of sample ILTf<sub>2</sub>NM50 and N<sub>2</sub> adsorption-desorption isotherms at 77 K on different samples. See DOI: 10.1039/c5ra07561k

Qing He and co-workers have published a review stating that the advantages that supported ionic liquids can bring to CO<sub>2</sub> capture has been a major focus in the field of CO<sub>2</sub> cycloaddition to epoxides.<sup>18</sup>

In the context of CCU the effects of both the cation and the anion of the supported ILs and their interactions with the solid supports for CO<sub>2</sub> capture and subsequent chemical conversion must be investigated together as well as the possibility of epoxide activation by remaining surface hydroxyl groups, as proposed by Cao *et al.*<sup>19</sup> This work aims to investigate the behavior of covalently grafted imidazolium ionic liquids in MCM-41 materials in both catalytic activity for propylene carbonate syntheses as well as the CO<sub>2</sub> sorption capacity and the role that different anions can perform on the solid surface when CO<sub>2</sub> sorption takes place, both experimentally and by electronic-structure numerical simulations.

The IL 1-methyl-3-(3-trimethoxysilylpropyl)imidazolium chloride ((MeO)<sub>3</sub>SipmimCl) was grafted in MCM-41 and subsequently [Cl<sup>-</sup>] anion was changed to [BF<sub>4</sub><sup>-</sup>], [PF<sub>6</sub><sup>-</sup>] or [Tf<sub>2</sub>N<sup>-</sup>]. For CO<sub>2</sub> cycloaddition reactions, the effect of changing reaction conditions such as temperature, pressure and time were studied as well as the effects of IL anion, IL concentration and the use of Lewis acidic co-catalyst. The recyclability of the catalytic systems was also evaluated.

## Results and discussion

### Catalyst/sorbent characterization

The IL modified MCM-41 materials were characterized and submitted to the CO<sub>2</sub> sorption tests as well as to the catalytic reactions aiming to obtain cyclic carbonates. The obtained samples were denominated according to the IL content and the anion present as described in Table 1.

The infrared spectrum of the MCM-41 presents a wide band at 3322 cm<sup>-1</sup> corresponding to the silanol  $\nu_{\text{OH}}$  and two bands at 1695 and 1637 cm<sup>-1</sup> assigned to  $\nu_{\text{Si-O}}$ , as well as the bands at 1163, 804 and 615 cm<sup>-1</sup> attributed to  $\nu_{\text{Si-O-Si}}$ . The assignments for samples of MCM-41 with supported ionic liquids with different anions are detailed in ESI, Table S1.† The assignments related to ionic liquids, especially imidazolium ring bands are in the range of 1570–1577 cm<sup>-1</sup> and 1460–1464 cm<sup>-1</sup> assigned to  $\nu_{\text{C-C}}$  and  $\nu_{\text{C-N}}$  and the alkyl chain approximately at 2934–2959 cm<sup>-1</sup> assigned to  $\nu_{\text{C-H}}$  of methyl and methylene. The bands corresponding to the ionic liquids anions are also well defined in the region between 1236–805 cm<sup>-1</sup>. It is noteworthy

to mention that the siloxane bands  $\nu_{\text{Si-O-Si}}$ , in the range of 1126–1182 cm<sup>-1</sup> and disiloxane band  $\nu_{\text{R}_3\text{Si-O-SiR}_3}$  in the range of 1047–1070 cm<sup>-1</sup>, are ascribed to the chemical bonds between silicon and IL indicating the successful grafting of the IL into the material.<sup>20–23</sup>

The thermal analyses indicated that the pure ILs are stable up to 773.15 K, when its total decomposition occurs. For the support any degradation event was observed until 1273.2 K. When the ILs are grafted into MCM-41 only one degradation step is observed around 673.15 K evidencing a lower degradation temperature when compared to pure ILs. The decomposition temperatures of ILs are well separated from those of the solid support allowing to evaluate the grafted IL content on the support. For all samples with a theoretical value of 20% IL content, the determined value by thermal analyses was in good agreement, *e.g.*, ILCIM20 was 22.3% in TGA and for ILCIM50 was 33.7%. On the other side for samples with a theoretical amount of 50% IL the thermal analyses results evidenced only 30%, indicating that this might be the maximum amount of IL that can be grafted. See as example the thermal analysis for sample ILTf<sub>2</sub>NM50 ESI, Fig. S1.†

Fig. 1 presents the <sup>29</sup>Si-CPMAS NMR spectra for MCM-41 and ILBF<sub>4</sub>M50 samples as an example. Both spectra show two <sup>29</sup>Si peaks at chemical shift at *ca.* -101 and -110 ppm assigned to Q<sup>3</sup> and Q<sup>4</sup> environments, respectively, from MCM-41. The <sup>29</sup>Si chemical shifts at *ca.* -60 and -68 ppm of modified MCM-41 (Fig. 1b) correspond to T<sup>2</sup> and T<sup>3</sup> silicon sites, respectively, as a result of the covalent bonding of the IL at the pore wall. T sites are formed at the expense of Q<sup>3</sup> sites as observed in Fig. 1. The assignment made here is also in good agreement with the literature.<sup>23–26</sup>

The XRD patterns of the MCM-41 (Fig. 2(a)) and the sample MCM-41 grafted with IL (as an example sample ILTf<sub>2</sub>NM50 Fig. 2(b)) shows an ordered, crystalline structure.<sup>27</sup> The well-defined pore structures are confirmed by the presence of high-angle reflections corresponding to (110), (200), and (210) planes.<sup>27,28</sup>

The results obtained for all samples of modified MCM-41 presented similar XRD patterns confirming that the MCM-41 crystalline structures were unaffected upon IL grafting.

The N<sub>2</sub> adsorption-desorption isotherms of all samples are type IV according to the IUPAC classification for adsorption isotherms<sup>29</sup> indicating the presence of mesoporosity ESI, Fig. S2.†<sup>28,30</sup> Table 2 shows the physical characterization of the studied adsorbents. The data demonstrates that the surface

Table 1 Prepared solids denomination accordingly anion and amount of grafted IL

| Supported ionic liquid   | IL (% w/w) | Acronym                |
|--|------------|------------------------|
| 1-Methyl-3-(trimethoxysilylpropyl)-imidazolium chloride                          | 20         | ILCIM20                |
| 1-Methyl-3-(trimethoxysilylpropyl)-imidazolium chloride                          | 50         | ILCIM50                |
| 1-Methyl-3-(trimethoxysilylpropyl)-imidazolium tetrafluoroborate                 | 50         | ILBF <sub>4</sub> M50  |
| 1-Methyl-3-(trimethoxysilylpropyl)-imidazolium hexafluorophosphate               | 50         | ILPF <sub>6</sub> M50  |
| 1-Methyl-3-(trimethoxysilylpropyl)-imidazolium bis(trifluoromethylsulfonyl)imide | 20         | ILTf <sub>2</sub> NM20 |
| 1-Methyl-3-(trimethoxysilylpropyl)-imidazolium bis(trifluoromethylsulfonyl)imide | 50         | ILTf <sub>2</sub> NM50 |

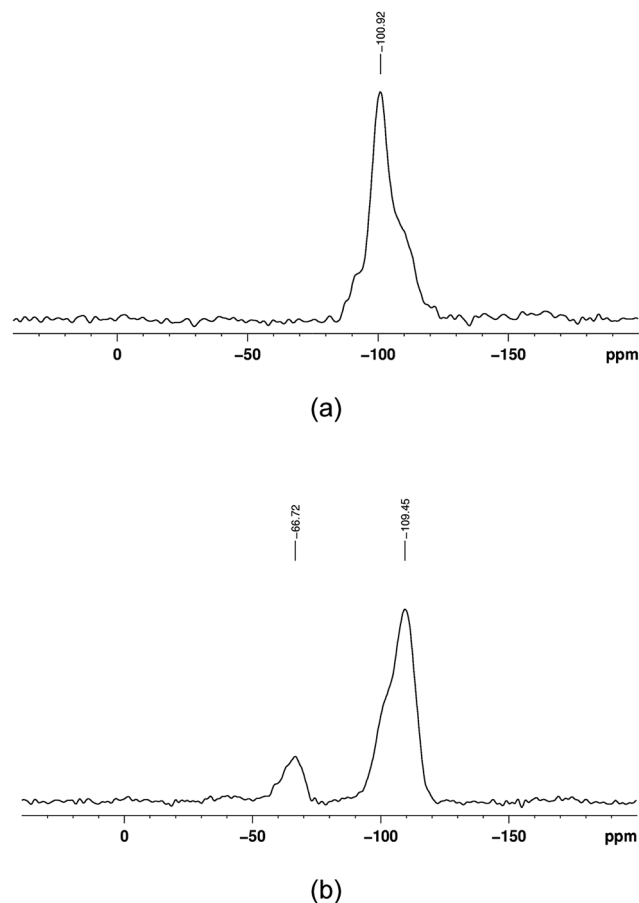


Fig. 1  $^{29}\text{Si}$  CPMAS NMR spectra of (a) MCM-41 and (b) ILBF<sub>4</sub>M50 (modified MCM-41).

area of MCM-41 decreases around 70% when the IL (MeO)<sub>3</sub>-SipmimCl was immobilized. When the anion exchange was performed this effect was even more important reaching a surface area value of 9.39 m<sup>2</sup> g<sup>-1</sup> to ILBF<sub>4</sub>M50. These results evidenced that the IL covers the surface of the mesoporous MCM-41 materials and probably covers the material pores since its pore volume also decreases in the same order (approx. 66% when incorporating ILCIM50 and over 90% for ILBF<sub>4</sub>M50).

### Cycloaddition reactions

Regarding the CO<sub>2</sub> cycloaddition reactions, they were carried out by using synthesized materials; the reaction temperature and the use of ZnBr<sub>2</sub> as co-catalyst were evaluated. Table 3 presents the results for the cycloaddition reactions using the precursors MCM-41 and the neat IL (MeO)<sub>3</sub>SipmimCl as well as the modified MCM-41 materials with ILs with different anions. As it can be observed in Table 3 MCM-41 is not active on cycloaddition reactions. This behavior is expected because the material only exhibits in its structure Lewis acidic sites<sup>31</sup> (entry 1). The IL (MeO)<sub>3</sub>SipmimCl is active in this reaction with a conversion of 79.7% but with a low selectivity of 16% (see entry 2). The effect of temperature was also tested (383.15 K; 393.15 K and 403.15 K, entry 3, 4 and 5) and although a decrease

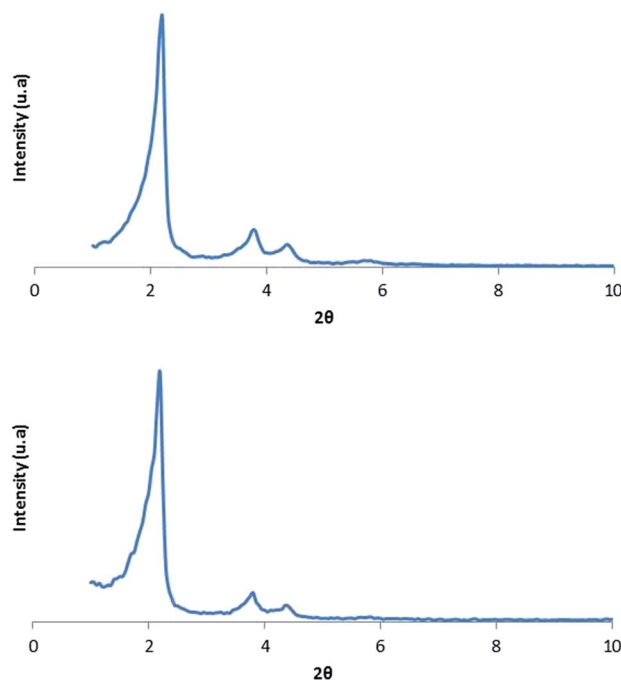


Fig. 2 XRD patterns of MCM-41 (a) and ILTF<sub>2</sub>NM50 (b).

of selectivity was observed from 96.0% (383.15 K) to 38.5% (403.15 K), the conversion efficiency was not altered. The same behavior was observed for ILs and poly(ILs). This is probably associated with the generation of side reactions such as PO isomerization and PC polymerization.<sup>10,32,33</sup> The use of ZnBr<sub>2</sub> enabled higher conversion values but lower selectivities (see entry 3 and 6). The increase in the conversion value is associated with the high Zn(II) reactivity combined with the high bromide nucleophilicity.<sup>11,34</sup> The results also evidence that ILCIM50 presented the best performance allying good conversion, selectivity and activity when compared to the others anions ([BF<sub>4</sub><sup>-</sup>], [PF<sub>6</sub><sup>-</sup>] and [TF<sub>2</sub>N<sup>-</sup>]). The activity depends on the inductive effect, diffusion limitation of residual pores and steric effect.<sup>28</sup> The [Cl<sup>-</sup>] anion also proved to be more active than [Br<sup>-</sup>] and [I<sup>-</sup>] in carbonate formation reaction, with the same quaternary ammonium salt as cation, due to their stronger nucleophilicity and structural volume when compared to the other anions.<sup>22</sup> The same ammonium based catalyst could perform synergistic effect with hydroxyl groups of inorganic oxides for epoxide activation, what could be also occurred in the

Table 2 Structural properties for supported ILs materials

| Samples                | $S_{\text{BET}}$ (m <sup>2</sup> g <sup>-1</sup> ) | $V_p$ (cm <sup>3</sup> g <sup>-1</sup> ) | $\rho_s^a$ (g cm <sup>-3</sup> ) |
|------------------------|--|--|----------------------------------|
| MCM-41                 | 841.7  | 0.95                                     | 0.340                            |
| ILCIM50                | 239.5  | 0.32                                     | 1.924                            |
| ILTF <sub>2</sub> NM50 | 233.7  | 0.25                                     | 1.493                            |
| ILPF <sub>6</sub> M50  | 120.7  | 0.26                                     | 1.913                            |
| ILBF <sub>4</sub> M50  | 9.39   | 0.048                                    | 2.115                            |

<sup>a</sup> Determined by helium picnometer.

Table 3 Catalyst screening for cycloaddition reactions<sup>a</sup>

| Entry | Catalyst/cocatalyst                      | Conversion% | Selectivity% | TON  |
|-------|--|-------------|--------------|------|
| 1     | MCM-41                                   | 0.0         | 0.0          | 0.0  |
| 2     | (MeO) <sub>3</sub> SipmimCl              | 79.7        | 16.0         | 53.1 |
| 3     | ILClM50                                  | 39.3        | 96.0         | 39.3 |
| 4     | ILClM50*                                 | 38.6        | 52.7         | 15.4 |
| 5     | ILClM50**                                | 41.9        | 38.5         | 16.8 |
| 6     | ILClM50/ZnBr <sub>2</sub>                | 67.0        | 75.0         | 44.6 |
| 7     | ILTf <sub>2</sub> NM50/ZnBr <sub>2</sub> | 14.6        | 38.0         | 18.2 |
| 8     | ILBF <sub>4</sub> M50/ZnBr <sub>2</sub>  | 62.2        | 65.0         | 41.5 |
| 9     | ILPF <sub>6</sub> M50/ZnBr <sub>2</sub>  | 41.9        | 79.0         | 27.9 |
| 10    | ILClM20/ZnBr <sub>2</sub>                | 41.3        | 47.0         | 51.6 |
| 11    | ILTf <sub>2</sub> NM20/ZnBr <sub>2</sub> | 7.9         | ND           | 9.8  |

<sup>a</sup> Reaction conditions: PO 100 mmol, catalyst 2.5 mmol, cocatalyst 0.625 mmol, initial CO<sub>2</sub> pressure 4.0 MPa, *t* = 6 h, *T* = 383.15 K, *T*\* = 393.15 K, *T*\*\* = 403.15 K TON = mmol of products per mmol of catalyst.

present case.<sup>19</sup> This result is important because the ILClM50 is the precursor material for the ILTf<sub>2</sub>NM50, ILBF<sub>4</sub>M50 and ILPF<sub>6</sub>M50, what is interesting both economically and environmentally.

The influence of the IL content was also evaluated and both the conversion and selectivity decreased with the increasing of the IL content (see entry 6, 7 and 10, 11).

The catalyst recyclability was evaluated, as highlighted in Fig. 3, and the conversion was slightly increased in the first two recycles probably due to the impurities withdrawal. After the fifth cycle a small conversion decrease is observed.

The main advantage of using grafted IL into mesoporous materials as catalyst is concerned with the PC separation by simple filtration. When pure ILs are used as catalysts a distillation step must be employed in the product purification protocol.<sup>10</sup>

### CO<sub>2</sub> sorption tests

The MCM-41 and the samples with ILs grafted on the MCM-41 surface carrying different anions were tested for CO<sub>2</sub> sorption and the results are presented in Fig. 4.

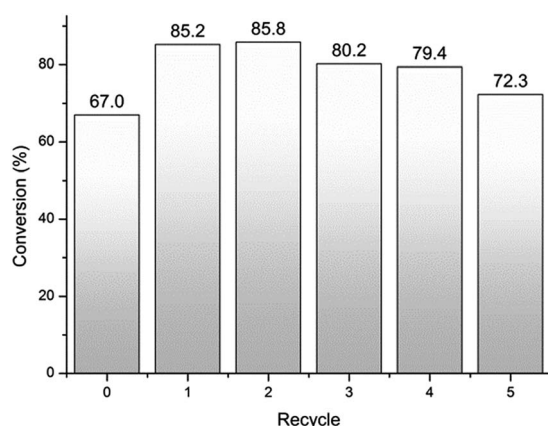
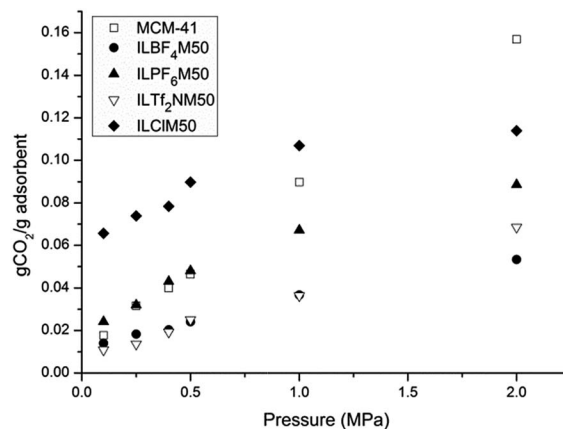


Fig. 3 Recycling experiments of ILCIM50.

Fig. 4 Adsorbed CO<sub>2</sub> for MCM-41 and MCM-41 supported ILs.

The ILCIM50 presented a higher sorption capacity up to 1 MPa of CO<sub>2</sub> pressure when compared to MCM-41 and all the other supported IL samples. For increasing pressures the MCM-41 presented better performance probably due to the effect of the higher surface area. The anion also plays an important role<sup>10</sup> and unlike what is observed for ionic liquids not supported, where fluorinated anions such as [TF<sub>2</sub>N<sup>-</sup>] present the best performance for CO<sub>2</sub> capture, the IL grafted with the [Cl<sup>-</sup>] anion gave the best results. This could be related to the structural volume of these anions, which prevent CO<sub>2</sub> sorption. The preferential affinity of imidazolium ILs with the [TF<sub>2</sub>N<sup>-</sup>] anion for CO<sub>2</sub> adsorption when compared to other less fluorinated anions is well documented in literature, being normally attributed to coulombic interaction established with CO<sub>2</sub> in the fluorinated anions.<sup>35</sup> Our results evidence that this trend is not conserved when the IL is supported since the best result was obtained for ILCIM50. In fact, the material with the [TF<sub>2</sub>N<sup>-</sup>] anion showed the poorest performance in comparison with the other supported ILs with the anions [Cl<sup>-</sup>], [BF<sub>4</sub><sup>-</sup>] and

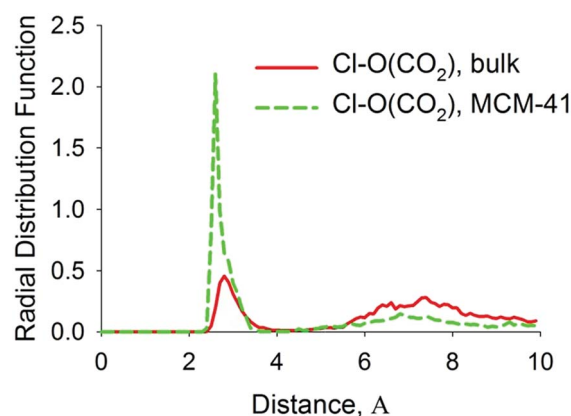


Fig. 5 Radial distribution functions computed for chloride anions and oxygen atoms of carbon dioxide in bulk 1,3-dimethylimidazolium chloride (solid red line) and in 1,3-dimethylimidazolium chloride adsorbed at the SiO<sub>2</sub> surface (green dashed line). The RDF normalization has been done in such a way, so that the integral of the entire function equals to unity.



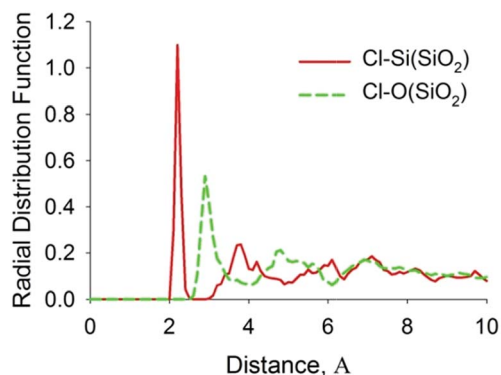


Fig. 6 Radial distribution functions computed for chloride anions and silicon atoms of  $\text{SiO}_2$  (solid red line); for chloride anions and oxygen atoms of  $\text{SiO}_2$  (green dashed line). The RDF normalization has been done in such a way, so that the integral of the entire function equals to unity.

$[\text{PF}_6^-]$ . These results seem to indicate that for immobilized ILs the size and bulkiness of the anion  $[\text{Tf}_2\text{N}^-]$  are probably more important.

The better performance observed for  $[\text{Cl}^-]$  anion containing systems must be highlighted once the imidazolium chloride is usually precursor for materials containing the fluorinated anions. By using  $[\text{Cl}^-]$  less synthesis steps are required lowering processes costs, a very important issue in the development of an useful adsorbent.<sup>36</sup>

Another criterion for selecting  $\text{CO}_2$  sorbent materials is the  $\text{CO}_2$  adsorption capacity. When comparing our results with those reported in literature for MCM-41 in which PEI was incorporated,<sup>37</sup> the  $\text{CO}_2$  sorption at 0.1 MPa and 298.15 K values were 0.0273 g  $\text{CO}_2$  per g sorbent for pure MCM-41 and 0.0329 g  $\text{CO}_2$  per g sorbent with 50% of PEI.<sup>38</sup> Our results showed that a value of 0.0655 g  $\text{CO}_2$  per g sorbent was reached with the sample ILClM50 at the same pressure and temperature, reaching 0.11 g  $\text{CO}_2$  per g sorbent at 1 MPa, equivalent to 11% w/w.

### Atomistic-level interpretation of the experimental observations

The reported experimental results are non-intuitive, as chloride anion was not expected to exhibit the best  $\text{CO}_2$  capturing ability based on the results obtained for the neat imidazolium-based chloride. To rationalize the experimental results we employed the state-of-the-art atomistic-precision simulation method, PM7-MD,<sup>39,40</sup> developed by us. The method was applied to locate free energy minimum of the RTIL-Cl +  $\text{CO}_2$  + MCM-41 system and unveil its structure. The PM7-MD method has shown its robustness and reliability in a few previous studies including those on ionic liquids.<sup>39,41,42</sup> The methodology is explained elsewhere.<sup>39,42</sup>

Two minor simplifications were made as compared to the experimental setups. First, imidazolium-based cation was presented as 1,3-dimethylimidazolium cation,  $[\text{MMIM}]^+$ , since its major  $\text{CO}_2$  capturing capacity is deemed to be linked to the imidazole ring. Second, the MCM-41 surface was simplistically represented as  $\text{SiO}_2$  nanoparticle,  $\text{Si}_{32}\text{O}_{64}$ . These assumptions

are important for computational efficiency of the scheduled numerical simulations. The PM7-MD trajectory was recorded during 50 ps, out of which the first 20 ps were regarded as equilibration and the remaining 30 ps were regarded as an equilibrium thermal motion at 300 K.

Fig. 5 compares simulated radial distribution functions (RDFs) between the chloride anion and carbon dioxide in the bulk  $[\text{MMIM}][\text{Cl}]$  and upon adsorption at the  $\text{SiO}_2$  surface. Indeed, correlation is a few times more significant in the presence of  $\text{SiO}_2$ . However, this observed correlation does not necessarily mean that the interaction strength between these particular chemical entities increases (in the sense of pairwise attraction force). The correlation can also be a result of both particles adsorption at the  $\text{SiO}_2$  surface, which restrains their mobility. Fig. 6 investigates adsorption of the chloride anion at the  $\text{SiO}_2$  surface. PM7-MD calculations suggests a strong adsorption at 300 K, whereas the closest-approach distance for the silicon–chlorine atom pair amounts to 2.1 Å. Such a small distance suggests a partial covalent bonding and, therefore, a high binding energy. Not all chloride anions join the surface though (Fig. 7). A few of them remain with the  $[\text{MMIM}]^+$  cations. Out of  $[\text{MMIM}][\text{Cl}]$  and  $\text{SiO}_2$ ,  $\text{CO}_2$  prefers  $\text{SiO}_2$ . Indeed, three  $\text{CO}_2$  molecules are in direct contact with the surface, whereas only one is within the ionic liquid media. This ratio persists

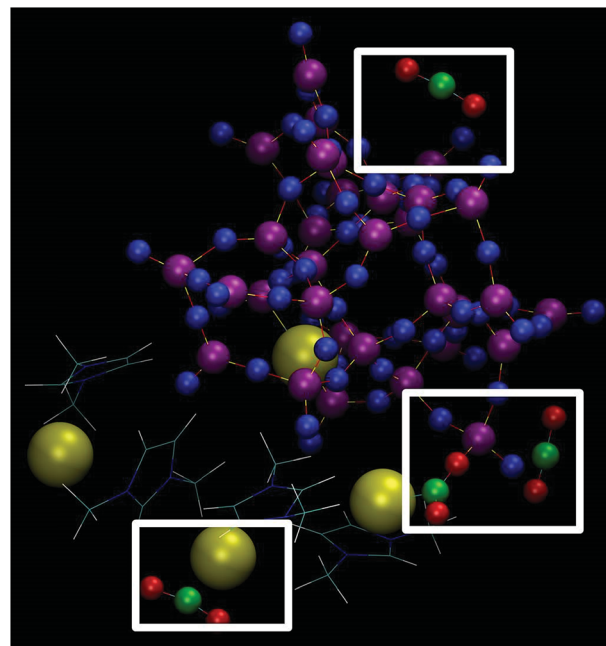


Fig. 7 The immediate molecular configuration corresponding to free energy minimum at 300 K. Prior to taking this molecular snapshot, the ion-molecular system has been simulated during 30 ps with an integration time-step of 1.0 fs. White squares indicate principal interaction pattern in the considered system: chloride– $\text{CO}_2$  binding and  $\text{CO}_2$ – $\text{SiO}_2$  binding at finite temperature conditions. Chloride anions are yellow; oxygen and carbon atoms of  $\text{CO}_2$  are red and green; oxygen and silicon atoms of  $\text{SiO}_2$  are blue and purple. Note that the imidazolium-based cation (displayed as wires) poorly participates both in the  $\text{CO}_2$  capture (despite their intrinsically acidic hydrogen atom) and the adsorption on the  $\text{SiO}_2$  surface.

throughout the entire recorded PM7-MD trajectory. To recapitulate, we expect MCM-41 to exhibit better CO<sub>2</sub> binding ability than chloride containing imidazolium-based RTILs.

Based on the experimental data and numerical simulations, we envision two major reasons of why chloride overperforms other anions when adsorbed at MCM-41. First, chloride is relatively small (as compared to other anions). It cannot occupy all the available binding sites of MCM-41. Other ions, in turn, adsorb at the MCM-41 surface and prevent CO<sub>2</sub> from populating the corresponding binding sites. Second, chloride interacts strongly with the imidazolium cation and is, due to this reason, incapable to join the SiO<sub>2</sub> surface. Other anions, with more delocalized charge density, are more mobile and populate the binding sites more readily.

The performed PM7-MD simulations provide an interpretation of the experimental observations on the CO<sub>2</sub> absorption in the considered three-component systems featuring a variety of ion-molecular interactions. According to our simulations, MCM-41 is a primary driver of CO<sub>2</sub> capture. Furthermore, it exhibits a good binding with the anions constituting ionic liquids, particularly with chlorine based ILs.

## Experimental

### Chemicals

1-Methylimidazole (Aldrich, 99.0%), 3-chloropropyltrimethoxysilane (Aldrich, 97.0%), LiTf<sub>2</sub>N (Aldrich, 99.0%), toluene (Merck, 99.9%), acetone (Vetec, 99.5%), dichloromethane (Vetec, 99.5%), diethyl ether (AGA, 95.0%), MgSO<sub>4</sub> (Acros Organics, 97.0%), propylene oxide (Aldrich, 99%), CO<sub>2</sub> (air liquids/99.998%). The solvents were dried before the synthesis. The support MCM-41, aluminosilicate mesoporous, was purchased from Sigma Aldrich and calcinated at 773.15 K for 12 hours before use.

### Ionic liquid synthesis

1-Methyl-3-(3-trimethoxysilylpropyl)imidazolium chloride was synthesized by the reaction of 1-methylimidazole with 3-chloropropyl trimethoxysilane (molar ratio 1 : 1.5) under reflux in toluene and nitrogen atmosphere for 48 h, following literature.<sup>43–46</sup> After that, the reaction mixture was cooled down to room temperature and the organic upper phase separated. The resulting product was a yellow viscous ionic liquid. The ionic liquid phase was then washed with diethyl ether. Finally, the obtained product was dried at 323.15 K for 8 h. The structure of the IL (MeO)<sub>3</sub>SipmimCl was confirmed by <sup>1</sup>H-NMR and FTIR.

<sup>1</sup>H-NMR (400 MHz, CDCl<sub>3</sub>, 298.15 K) δ (ppm): 0.58 (m, CH<sub>2</sub>Si), 1.91 (m, CH<sub>2</sub>CH<sub>2</sub>N), 3.49 (s, SiOCH<sub>3</sub>), 3.63 (s, CH<sub>3</sub>N), 4.06 (t, CH<sub>2</sub>N), 4.27 (t, CH<sub>2</sub>), 7.39 (s, H5), 7.61 (s, H4), 10.39 (s, H2).

FTIR ν(cm<sup>-1</sup>): 3031, Si-O; 2944–2839 for aliphatic C-H stretching (methyl and methylene groups); 1570–1457 C=C stretching and C-N of the imidazolium ring; 1175–1071 Si-OCH<sub>3</sub>; 805 from chloride anion.

### Ionic liquids immobilization

The grafting method consisted in the anchorage of the ionic liquid *via* cation. In a distillation apparatus, the MCM-41 was dispersed in dried toluene. After this (MeO)<sub>3</sub>SipmimCl (50% and 20%) was added and the mixture was stirred at 363.15 K for 16 h. In the following step, the solvent (toluene) and the byproduct methanol were distilled off. The excess of 1-methyl-3-(3-trimethoxysilylpropyl)imidazolium chloride was removed by extraction with boiling dichloromethane and the remaining solid dried under vacuum by 24 h. The dried support was then added to a solution of NaBF<sub>4</sub>, NaPF<sub>6</sub> or LiTf<sub>2</sub>N in acetone and left stirring from 24 h to 120 h at room temperature. After filtration, the excess of salt was removed by extraction with boiling CH<sub>2</sub>Cl<sub>2</sub> in a Soxhlet apparatus and the material was dried under reduced pressure,<sup>47</sup> as show in Fig. 8.

### Characterization

The FTIR spectra were collected on a Perkin-Elmer Spectrum 100 spectrometer in KBr pellet form. Thermal analyses were performed on TA Instrument equipment, model Q600 SDT. The TGA analyses were recorded ranging from room temperature to 1273.2 K for 30 min, with a heating rate of 10 °C min<sup>-1</sup> in a nitrogen atmosphere. NMR measurements were performed at room temperature on a Bruker Avance III 400 MHz spectrometer, for liquid and solid-state NMR for the observation of <sup>29</sup>Si resonances; cross-polarization magic angle spinning (CPMAS) at 5 kHz was selected to record silicon spectra. DRX analysis on Siemens D500 with radiation Cu Kα, λ = 1.54056 Å. The surface area and pore size calculated from nitrogen sorption data using Brunauer-Emmett-Teller (BET) at -196 °C (Micromeritics Instrument Corporation, TriStar II 3020 V1.03). The real density of powdered MCM-41 (ρ<sub>s</sub>) was determined on Ultrapycnometer 1000 – Quantachrome Corporation, volume cell of 20.45 cm<sup>3</sup> and pressure of 21.0 psi (1.45 bar).

### Cycloaddition reactions

The syntheses of propylene carbonate (PC) from CO<sub>2</sub> and propylene oxide (PO) were carried out in the presence of the supported imidazolium-based ILs combined with the different anions [Cl<sup>-</sup>], [BF<sub>4</sub><sup>-</sup>] and [Tf<sub>2</sub>N<sup>-</sup>]. All cycloaddition reactions were performed in a 120 cm<sup>3</sup> stainless steel autoclave equipped

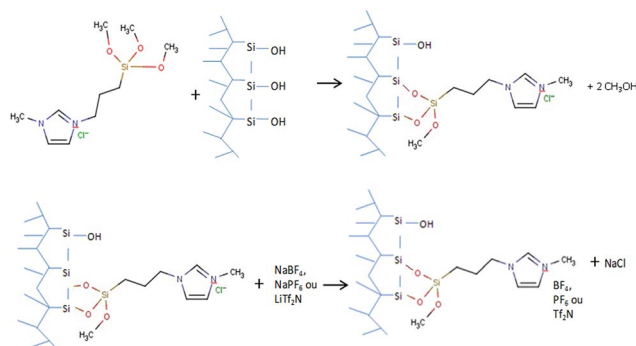


Fig. 8 Scheme of ILs immobilization on MCM-41.

with magnetic stirring. For a typical reaction, 100 mmol of propylene oxide, 2.5% mol of supported ionic liquid and 0.625 mmol of ZnBr<sub>2</sub> were used.

The experimental parameters assessment started with reaction temperature (383.15 K, 393.15 K and 403.15 K) for the sample ILCIM50 at 4.0 MPa and 6 h. From the optimal temperature the use of metal halide as co-catalyst (ZnBr<sub>2</sub>) was tested.

The syntheses were performed without any additional solvent. The autoclave was pressurized with CO<sub>2</sub> and heated to the desired working temperature. After reaction completion, the reactor was cooled to room temperature and slowly depressurized. The separation of the catalyst from propylene carbonate was performed by a simple filtration. The resulting liquid mixtures were analyzed using a gas chromatograph Shimadzu GC14B equipped with a flame ionization detector (FID) and a DB-5HT column (15 m × 0.32 mm × 0.10 μm) using acetophenone as internal standard and diethyl ether as solvent.

### CO<sub>2</sub> adsorption measurements

The sorption of CO<sub>2</sub> in the samples were gravimetrically assessed in a Magnetic Suspension Balance (MSB), (Rubotherm Prazisionsmesstechnik GmbH, 35 MPa and 673.15 K) equipped with a single sinker device for absorbate density determination and thermostated with an oil bath (Julabo F25/± 273.16 K). The apparatus details are well described elsewhere.<sup>48,49</sup> When compared to other gravimetric sorption methods, the MSB device has the advantage of allowing high pressure sorption measurements since the sample can be potted into a closed chamber coupled to an external precise balance (accuracy of ±10 μg). The samples (0.06 to 0.09 g) were weighted and transferred to the MSB sample container, and the system was subjected to a 10<sup>-7</sup> MPa vacuum at the temperature of the sorption measurement, 298.15 K, for 24 hours (constant weight was achieved in this time). The CO<sub>2</sub> (air liquids/99.998%) was admitted into the MSB pressure chamber up to the desired pressure, 0.1–2 MPa in this study, pressure gauge with an accuracy of 10<sup>-3</sup> MPa was used to control the system pressure. The solubility of CO<sub>2</sub> in the samples for each isotherm and pressure considered was measured 3–4 hours after no more weight increasing for CO<sub>2</sub> sorption was observed. At this step of CO<sub>2</sub> solubility in the samples, the weight reading from the microbalance at pressure *P* and temperature *T* is recorded as *W*<sub>t</sub>(*P*, *T*). The mass of dissolved CO<sub>2</sub> in the sample (*W*<sub>absolute</sub>) was calculated using the following eqn (1):

$$W_{\text{absolute}} = [W_t(P, T) - W_{\text{sc}}(P, T) + \rho_g(P, T)(V_{\text{sc}}(T) + V_s(T) + V_{\text{ads}}) - W_s(\text{vac}, T)] \quad (1)$$

where *W*<sub>sc</sub>(*P*, *T*) is the weight of sample container,  $\rho_g(P, T)$  stands for CO<sub>2</sub> density, directly measured with the MSB coupled single-sinker device, *V*<sub>sc</sub>(*T*) is the volume of the sample container, determined from a buoyancy experiment when no sample is charged into the sample container, *V*<sub>s</sub>(*T*) the specific solid sample volume, *W*<sub>s</sub>(*vac*, *T*) is the weight of samples under vacuum and the term  $\rho_g(P, T)(V_{\text{sc}}(T) + V_s(T))$ , represents the buoyancy force.

The volume of the adsorbed phase *V*<sub>ads</sub> has to be taken into account in the buoyancy correction for determination of absolute gas adsorption. In this paper the density of the adsorbed phase  $\rho_{\text{ads}}$  was assumed to be the density of liquid CO<sub>2</sub> in a reference state (boiling point at 1 atm) and the *V*<sub>ads</sub> was obtained by dividing the adsorbed mass, *m*<sub>ads</sub> by the density of the adsorbed phase,  $\rho_{\text{ads}}$ . Further details on data handling from the adsorption isotherms measured may be found in literature.<sup>49</sup>

## Conclusions

We have shown that IL with [Cl<sup>-</sup>] anion supported in MCM-41 works as an efficient CO<sub>2</sub> sorbent and catalyst for CO<sub>2</sub> transformation. These materials present a good thermal stability and when applied as catalyst can easily be separated from the reaction medium. For CO<sub>2</sub> sorption appears as an alternative to the use of liquid solvents. Another point to emphasize is that unlike ILs the solid material ILCIM50 with the [Cl<sup>-</sup>] anion is the best choice for both CO<sub>2</sub> capture and conversion appearing as a good option for an integrated process of CO<sub>2</sub> capture-conversion. Based on the experimental data and numerical simulations, we presented the two major reasons of why chloride overperforms other anions when adsorbed at MCM-41.

## Acknowledgements

AA thanks CAPES (process no. 9259120) and JB thanks CNPq (PIBIC 3475) for scholarships and SE and RL thanks CNPq for DT scholarship. V. V. C. acknowledges research grant from CAPES under the "Science Without Borders" program. We thank Michèle Oberson de Souza (Universidade Federal do Rio Grande do Sul, Porto Alegre, Brazil) for the Nitrogen adsorption analysis and X-Ray Diffraction analysis. L. M. thank the Portuguese NMR Network (RNRMN) and CICECO-Aveiro Institute of Materials (Ref. FCT UID/CTM/50011/2013), financed by national funds through the FCT/MEC and when applicable co-financed by FEDER under the PT2020 Partnership Agreement.

## Notes references

- 1 P. Markewitz, W. Kuckshinrichs, W. Leitner, J. Linssen, P. Zapp, R. Bongartz, A. Schreiber and T. E. Müller, *Energy Environ. Sci.*, 2012, **5**, 7281.
- 2 W. Cheng, B. Xiao, J. Sun, K. Dong, P. Zhang, S. Zhang and F. T. T. Ng, *Tetrahedron Lett.*, 2015, **56**, 1416.
- 3 M. J. Muldoon, S. N. V. K. Aki, J. L. Anderson, J. K. Dixon and J. F. Brennecke, *J. Phys. Chem. B*, 2007, **111**, 9001.
- 4 M. Hasib-ur-Rahmana, M. Siaj and F. Larachi, *Chem. Eng. Process.*, 2010, **49**, 313.
- 5 J. L. Anthony, E. J. Maginn and J. F. Brennecke, *J. Phys. Chem. B*, 2002, **106**, 7315.
- 6 X. Zhang, X. Zhang, H. Dong, Z. Zhao, S. Zhang and Y. Huang, *Environ. Sci. Technol.*, 2012, **5**, 6668.
- 7 J. Peng and Y. Deng, *New J. Chem.*, 2001, **25**, 639.
- 8 J. Sun, S. Fujita and M. Arai, *J. Organomet. Chem.*, 2005, **690**, 3490.

- 9 J. Sun, R. Liu, S. Fujita and M. Arai, Ionic Liquids in Green Carbonate Synthesis, in *Ionic Liquids – Classes and Properties*, ed. Scott T. Handy, Intech Open Access Publisher, Rijeka, 2011, pp. 273–310.
- 10 A. Aquino, F. L. Bernard, M. O. Vieira, J. V. Borges, M. F. Rojas, F. Dalla Vecchia, R. Ligabue, M. Seferin, S. Menezes and S. Einloft, *J. Braz. Chem. Soc.*, 2014, **25**, 2251.
- 11 W. Cheng, Q. Su, J. Wang, J. Sun and T. T. Flora, *Catalysts*, 2013, **3**, 878–901.
- 12 H. Sun and D. Zhang, *J. Phys. Chem. A*, 2007, **111**, 8036–8043.
- 13 F. Karadas, M. Atilhan and S. Aparício, Review on the Use of Ionic Liquids (ILs) as Alternative Fluids for CO<sub>2</sub> Capture and Natural Gas Sweetening, *Energy Fuels*, 2010, **24**, 5817–5828.
- 14 T. C. Drage, J. M. Blackman, C. Pevida and C. E. Snape, *Energy Fuels*, 2009, **23**, 2790.
- 15 J. D. Carruthers, M. A. Petruska, E. A. Sturm and S. M. Wilson, *Microporous Mesoporous Mater.*, 2011, **154**, 62.
- 16 J.-R. Li, Y. Ma, M. C. McCarthy, J. Sculley, J. Yu, H.-K. Jeong, P. B. Balbuena and H.-C. Zhou, *Coord. Chem. Rev.*, 2011, **255**, 1791–1823.
- 17 M. Rezakazemi, A. E. Amooghini, M. M. Montazer-Rahmati, A. F. Ismail and T. Matsuura, *Prog. Polym. Sci.*, 2014, **39**, 817.
- 18 Q. He, J. W. Ó'Brien, K. A. Kitselman, L. E. Tompkins, G. C. T. Curtis and F. M. Kerton, *Catal. Sci. Technol.*, 2014, **4**, 1513.
- 19 T. Cao, L. T. Sun, Y. Shi, L. Hua, R. Zhang, L. Guo, W. W. Zhu and Z. S. Hou, *Chin. J. Catal.*, 2012, **33**, 416.
- 20 A. Lesniewski, J. Niedziolka, B. Palys, C. Rizzi, L. Gaillon and M. Opallo, *Electrochem. Commun.*, 2007, **9**, 2580.
- 21 G. A. Eimer, M. B. Gómez Costa, L. B. Pierella and O. A. Anunziata, *J. Colloid Interface Sci.*, 2003, **263**, 400.
- 22 R. R. Sever, R. Alcalá, J. A. Dumesic and T. W. Root, *Microporous Mesoporous Mater.*, 2003, **66**, 53.
- 23 X. S. Zhao, G. Q. Lu, A. K. Whittaker, G. J. Millar and H. Y. Zhu, *J. Phys. Chem. B*, 1997, **101**, 6525.
- 24 J. Trebosc, J. W. Wiench, S. Huh, V. S. Y. Lin and M. Pruski, *J. Am. Chem. Soc.*, 2005, **127**, 3057.
- 25 P. R. S. Braga, A. A. Costa, J. L. Macedo, G. F. Ghesti, M. P. Souza, J. A. Dias and S. C. L. Dias, *Microporous Mesoporous Mater.*, 2011, **139**, 74.
- 26 J. Cejka, N. Zilková and P. Nachtigall, *Proceedings of the 3rd international zeolite symposium (3 rd FEZA)*, Prague, Czech Republic, 2005.
- 27 U. Ciesla and F. Schüth, *Microporous Mesoporous Mater.*, 1999, **27**, 131.
- 28 S. Udayakumar, M. Lee, H. Shim, S. Park and D. Park, *Catal. Commun.*, 2009, **10**, 659.
- 29 Y. Belmabkhout, R. Serna-Guerrero and A. Sayari, *Chem. Eng. Sci.*, 2009, **64**, 3721.
- 30 S. J. Gregg and K. S. W. Sing, *Adsorption, surface area and porosity*, London: Academic Press, United States of America, 1982, p. 303.
- 31 E. Armengol, M. L. Cano, A. Corma, H. Garcia and M. T. Navarro, *J. Chem. Soc., Chem. Commun.*, 1995, **5**, 519.
- 32 M. F. Rojas, F. L. Bernard, A. J. Borges, F. Dalla Vecchia, S. Menezes, R. Ligabue and S. Einloft, *J. Mol. Catal. A: Chem.*, 2014, **392**, 83.
- 33 T. Sakakura, J. Choi and H. Yasuda, *Chem. Rev.*, 2007, **107**, 2365.
- 34 L. Xiao, F. Li, J. Peng and C. Xia, *J. Mol. Catal. A: Chem.*, 2006, **253**, 265.
- 35 J. Zhang, J. Sun, X. Zhang, Y. Zhao and S. Zhang, *Greenhouse Gases: Sci. Technol.*, 2011, 142.
- 36 A. Samanta, A. Zhao, G. K. H. Shimizu, P. Sarkar and R. Gupta, *Ind. Eng. Chem. Res.*, 2012, **51**, 1438.
- 37 X. Xu, X. Zhao, L. Sun and X. Liu, *J. Nat. Gas Chem.*, 2009, **18**, 167.
- 38 X. Xu, C. Song, J. M. Andrésen, B. G. Miller and A. W. Scaroni, *Microporous Mesoporous Mater.*, 2003, **62**, 29.
- 39 V. Chaban, *Chem. Phys. Lett.*, 2014, **613**, 90.
- 40 J. J. P. Stewart, *J. Mol. Model.*, 2013, **19**, 1.
- 41 V. Chaban, *Chem. Phys. Lett.*, 2015, **618**, 46.
- 42 V. Chaban, *Chem. Phys. Lett.*, 2015, **618**, 89.
- 43 B. Karimi and D. Enders, *Org. Lett.*, 2006, **8**, 1237.
- 44 H. Valizadeh, M. Amiri and A. Shomali, *C. R. Chim.*, 2011, **14**, 1103.
- 45 R. Amini, A. Rouhollahi, M. Adibi and A. Mehdinia, *J. Chromatogr. A*, 2011, **1218**, 130.
- 46 M. Valkenberg, C. Castro and W. Hölderich, *Green Chem.*, 2001, **4**, 88–93.
- 47 A. Blasig, J. Tang, X. Hu, Y. Shen and M. Radosz, *Fluid Phase Equilib.*, 2007, **256**, 75.
- 48 F. Dreisbach and H. W. Losch, *J. Therm. Anal. Calorim.*, 2000, **62**, 515.
- 49 F. Dreisbach and H. W. Losch, *Adsorption*, 2002, **8**, 95.